

## Relative Photoreactivity of 5,7-Dimethoxycoumarin and *cis-syn* 8-MOP $\langle \begin{smallmatrix} 4',5' \\ 5',6' \end{smallmatrix} \rangle$ Thd Monoadduct to Thymidine in a Dry Film State

Sang Chul Shim\* and Ho Kwon Kang

Department of Chemistry, Korea Advanced Institute of Science and Technology, Seoul 131

Received April 7, 1986

The photocycloaddition reactivity of 5,7-dimethoxycoumarin (DMC) to thymidine is much higher than that of *cis-syn* 8-methoxypsoralen  $\langle \begin{smallmatrix} 4',5' \\ 5',6' \end{smallmatrix} \rangle$  thymidine monoadducts, due to the steric effect. The different rate is also due to the relative reactivity of the singlet rather than the triplet excited state of the compounds. The biadducts of 8-methoxypsoralen and thymidine are first splitted into 4',5'-monoadducts and thymidine, not into 3,4'-monoadducts and thymidine by 254 nm light.

### Introduction

The photosensitizing ability of furocoumarins (psoralens) is generally correlated with their photoreactivity toward the pyrimidine bases, especially thymine, of DNA through [2+2] cycloaddition reaction.<sup>1-3</sup> One psoralen molecule intercalated in duplex DNA can successively photoreact with two pyrimidine bases to form interstrand cross-links. The cross-link is caused by the formation of cyclobutane adducts which arise from [2+2] cycloaddition of the psoralen 3,4- and 4',5'-double bonds with 5,6-double bonds of two pyrimidine bases.<sup>4,5</sup> The 4',5'-monoadducts absorb long wavelength UV light upto 380 nm whereas the 3,4-monoadducts absorb light only upto 320 nm. It is thus obvious that after the first quantum of near UV-light has been absorbed by the psoralen itself to form a monoadduct, the second quantum has to be absorbed by a 4',5'-monoadduct rather than 3,4-monoadducts, to form a cross-link. It is, therefore, very important to understand the reactivity of 4',5'-monoadduct to thymidine for the elucidation of photobiological activities of furocoumarins.

8-Methoxypsoralen(8-MOP), which has been the most used furocoumarin in the photochemotherapy of psoriasis<sup>6</sup>, is a well known photosensitizing agent. However, undesirable side effects such as carcinoma development have been reported.<sup>7</sup> 5,7-Dimethoxycoumarin (DMC) with only one functional group (pyrone double bond) strongly intercalate into DNA and has been shown to be highly lethal in *Bacillus subtilis rec* and *hcr* strains<sup>8,9</sup>, although most monofunctional coumarin derivatives were inactive. We have previously isolated and characterized the major photocycloadducts of DMC<sup>10</sup> and 8-MOP<sup>11-13</sup> to thymidine in a dry film state, respectively. To estimate the second stage photoreaction causing interstrand cross-link of DNA, photoreaction of the *cis-syn* 8-MOP  $\langle \begin{smallmatrix} 4',5' \\ 5',6' \end{smallmatrix} \rangle$  thymidine (F-2) and DMC to thymidine was carried out and their relative reactivity is examined.

### Materials and Methods

**Materials.** 8-Methoxypsoralen and thymidine were purchased from Sigma Chemical Company and used without further purification and DMC (Aldrich Chemical Company) was purified by recrystallization from ethanol. The *cis-syn* 8-MOP  $\langle \begin{smallmatrix} 4',5' \\ 5',6' \end{smallmatrix} \rangle$  Thd monoadducts (F-2) were prepared by

photolysis of a mixture of 8-MOP and thymidine in a dry film state as previously described<sup>11</sup> and isolated according to the procedure reported.<sup>12</sup> Kiesel Gel GF<sub>254</sub> (Merck) and Kiesel Gel 60(Merck, 230-400 mesh) were used for silica gel thin layer and flash column chromatography, respectively. Chromatographic grade solvents were used for high performance liquid chromatographic analysis.

**HPLC and Lobar Column Chromatography.** High performance liquid chromatography was performed on a Waters Associates Model 244 liquid chromatograph equipped with Model 600A solvent delivery system, Model 440 UV absorbance detector, Model U6K Universal injector, and Model 660 solvent programmer.

Analytical liquid chromatography was utilized in the analysis of photoproducts of DMC and thymidine under the following conditions: column;  $\mu$ -Bondapak C<sub>18</sub> (3.9 mm ID  $\times$  30cm), solvent; H<sub>2</sub>O/CH<sub>3</sub>CN/THF (20/2/1 by volume), flow rate; 1.5 ml/min, detector; UV (254nm).

To isolate the DMC-thymidine photocycloadducts, excess unreacted thymidine and DMC were removed by silica gel flash column chromatography varying the solvent polarity and each component was separated by Lobar chromatography using the following condition: column; Lobar LiChroprep RP-8 (2.5cm ID  $\times$  30cm), solvent; H<sub>2</sub>O/CH<sub>3</sub>CN/THF (20/2/1, by volume), flow rate; 5.0 ml/min (with a Model 600A solvent delivery system), detector; UV (254nm).

The analysis of the irradiated mixture of 8-MOP  $\langle \begin{smallmatrix} 4',5' \\ 5',6' \end{smallmatrix} \rangle$  Thd monoadduct and thymidine was also carried out under the following condition: column; Radial-pak cartridge 5  $\mu$ -C<sub>18</sub> (8.0mm ID  $\times$  10cm), solvent; CH<sub>3</sub>OH/H<sub>2</sub>O gradient, flow rate; 2.0ml/min, detector; UV(254nm).

**Analysis and isolation of [2+2] photocycloadducts of DMC and thymidine.** Two modules of a Rayonet Photochemical Reactor (The Southern New England Ultraviolet Co.) Model RPR-100 were stacked together and arranged in a horizontal position allowing the photolysis of solid samples. Transparent mixture of DMC and thymidine obtained as a dry film<sup>10</sup> was irradiated with RUL-3500 Å lamps for about 40 min. The irradiated substances were dissolved in methanol and analyzed by HPLC and the [2+2] photocycloadducts were separated by a Lobar column chromatography.

**Determination of reaction rates of F-2 and DMC with thymidine in a dry film state.** The 4',5'-monoadduct (4.58mg)

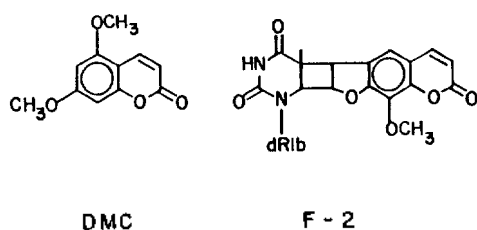


**Figure 1.** Structure of 5,7-dimethoxycoumarin(DMC) and 8-MOP- $\langle^{4,5}_{5,6}\rangle$ Thd(F-2).

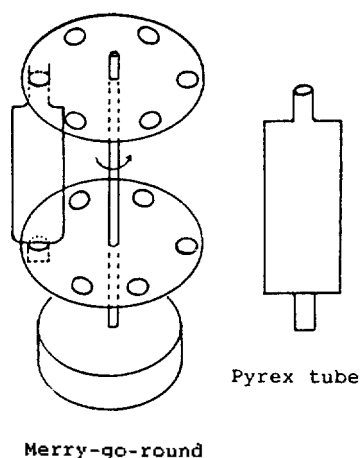


**Figure 2.** Irradiation apparatus for the kinetic study.

and 24.2mg of thymidine (molar ratio = 1:10) were dissolved in 100 ml of methanol. To minimize errors in the process of irradiation and extraction of photoreaction mixtures, a small portion (5ml) of the solution was delivered into each of several cylindrical pyrex tubes as shown in Figure 2. The Pyrex tubes containing the solution were rotated and heated to evaporate methanol off upto nearly dryness. The transparent substances formed as dry films on inner surface of the Pyrex tubes were irradiated for constant time intervals in a Rayonet photochemical reactor equipped with two RUL-3500Å lamps. The irradiated mixture was extracted with 2ml of methanol and this solution was used for HPLC analysis. Photoreaction of DMC and thymidine was carried out and analyzed by HPLC utilizing the same procedures.

## Results and Discussion

**Isolation and characterization of DMC-thymidine photocycloadducts.** The photoreaction mixture was analyzed by a high performance liquid chromatography. Eight stereoisomers can be produced in a [2+2] cycloaddition reaction of DMC and thymidine. Several peaks due to the photoadducts of DMC and thymidine appear between the retention times of thymidine and DMC (see Figure 3). These photoadducts were isolated by a flash column chromatography and separated by a Lobar LiChroprep RP-8 column chromatography. Each fraction collected was concentrated and lyophilized to obtain white solids. Ultraviolet-visible spectrum of each fraction shows a peak or shoulder at 273 nm or 276 nm. All the adducts yield DMC and thymidine on irradiation with 254 nm light, just like typical photosplitting of  $C_4$ -cyclooligomers of pyrimidine bases or DMC and DMC-thymine  $C_4$ -cycloadducts. DMC and thymidine regenerated were

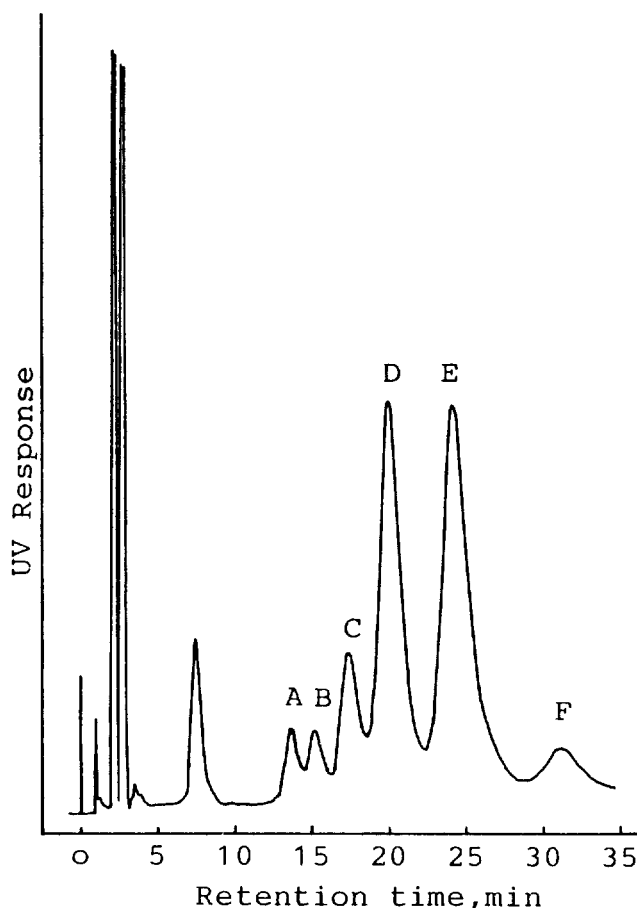


**Figure 3.** Analytical liquid chromatogram of photocycloadducts of 5,7-dimethoxycoumarin and thymidine.

detected by TLC analysis. The results indicate that fractions are different stereoisomers of  $C_4$ -cycloadducts of DMC and thymidine. IR spectra of two major products (D and E fractions) were obtained and they are consistent with those of authentic samples.<sup>10</sup>

**Isolation and characterization of F-2 and thymidine photoadducts: thymidine-8-MOP-thymidine biadducts.** The reaction mixture of F-2 and thymidine irradiated in a dry film state was analyzed by HPLC (see Figure 4). Numerous peaks appear except those responsible for F-2 and thymidine, and height of B-I peak increased along irradiation time. The photoproduct B-I was isolated and its UV spectrum is similar to that of [2+2] photocycloadduct of F-2 and tetramethylethylene.<sup>13</sup> B-I was analyzed under isocratic solvent system using  $H_2O/CH_3CN(6/1)$  by volume as eluent to observe two peaks and two shoulders. When B-I was irradiated with 254 nm, new peaks responsible for thymidine and F-2 appeared on TLC and HPLC chromatograms indicating that B-I products must be the [2+2] cycloadducts of F-2 and thymidine, *i.e.*, thymidine-8-MOP-thymidine biadducts. This also indicates that cyclobutane ring of pyrone side is photosplitted much faster than that of furan side.

**Comparison of photoreactivity of F-2 and DMC for thymidine.** F-2 and DMC in the presence of thymidine were irradiated in a dry film and solution states at constant time intervals, respectively. The decrease of absorbance (at 328nm) of F-2 and DMC along the irradiation time was estimated (Figures 5 and 6). The reaction mixtures were also analyzed

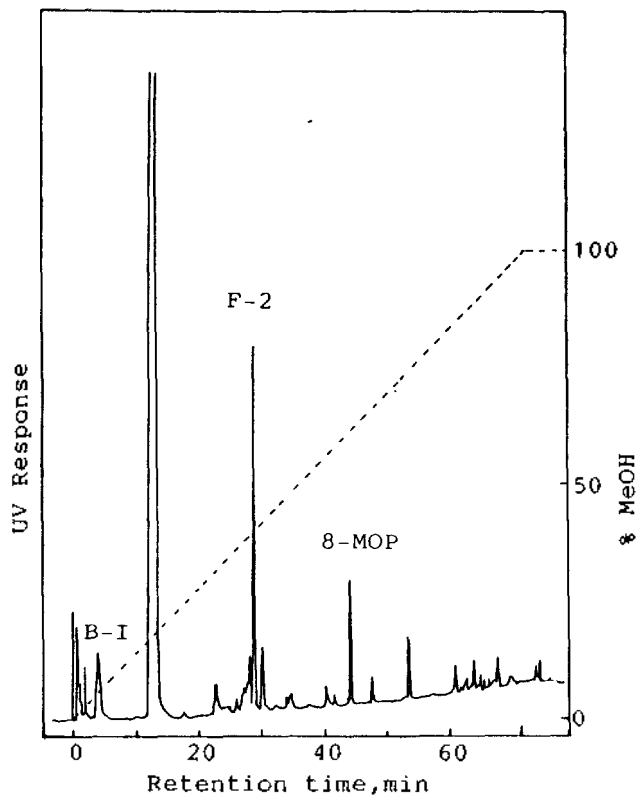


Figure 4. HPLC profile of photoproducts of F-2 and thymidine

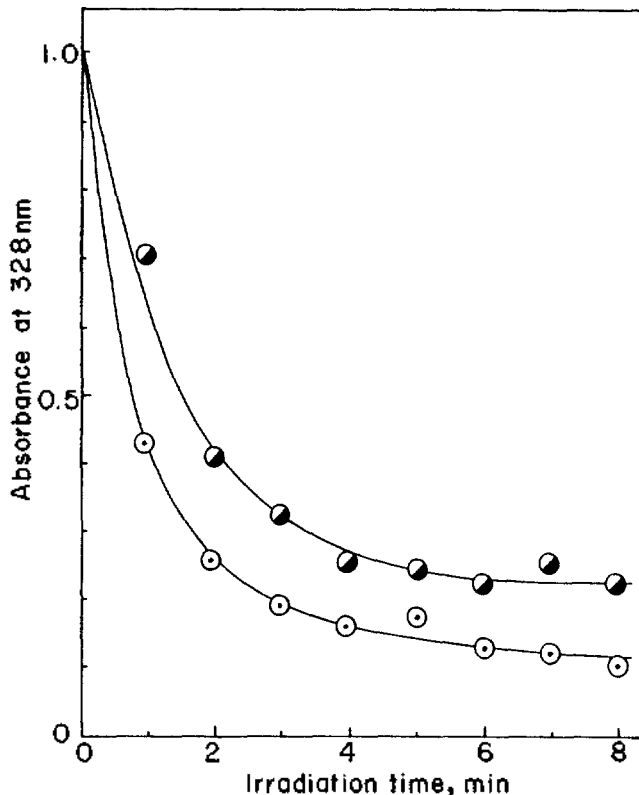


Figure 6. Disappearance rate of F-2(●) and DMC(○) in photoreaction with thymidine in a dry film state.

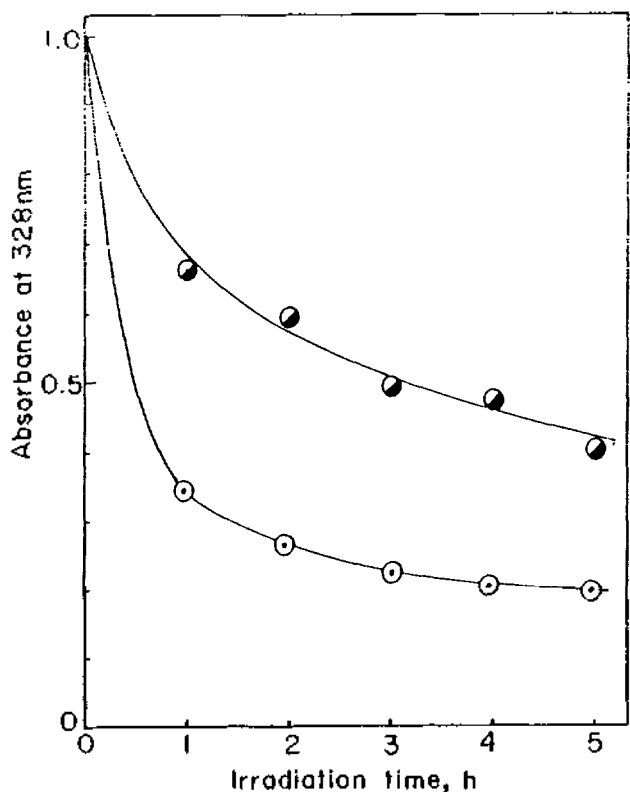


Figure 5. Disappearance rate of F-2(●) and DMC(○) in photoreaction with thymidine in a solution state.

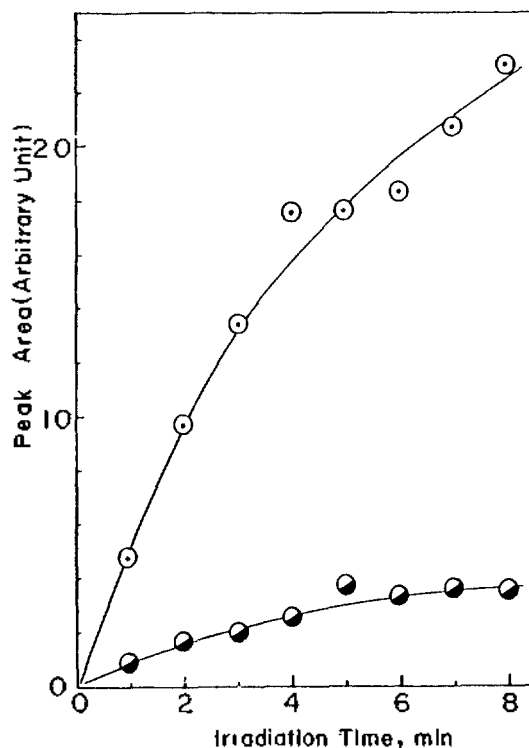


Figure 7. Relative rates of photocycloaddition reaction of F-2(●) and DMC(○) with thymidine in a dry film state.

by HPLC and area or height of the peaks responsible for F-2-thymidine and DMC-thymidine cycloadducts were measured with varying irradiation time (Figure 7). Both F-2

and DMC disappeared continuously in solution but thymidine adducts were not formed suggesting that the rate of adduct formation is much slower than the other decay processes of

the excited state in solution. On the other hand, faster disappearance of F-2 and DMC and C<sub>4</sub>-cycloadducts formation with thymidine were observed on irradiation in a dry film state in which diffusional encounters to form the adducts are not necessary. The effective thymidine concentration is higher in the dry film state than in solution by several orders of magnitude and the cycloaddition reaction rate is therefore enhanced in a film state. DMC disappears faster than F-2 in both dry film and solution states, and the rate of DMC-thymidine adduct formation is much greater than that of F-2 probably due to the steric factor in complexation with thymidine. In a dry film state, F-2 and DMC can form complexes with thymidine arranged properly in up and down sides of their molecular planes. Although both sides of molecular plane in DMC are available for complexation with thymidine, only one side in F-2 is available because of the bulky thymidine moiety with *cis-syn* stereochemistry. The different reactivity can be also attributed to the electronic factor. The reactivity of excited singlet state of DMC to tetramethylethylene is much greater than that of F-2 in solution and the ratio of phosphorescence to fluorescence quantum yields of F-2(0.68) is greater than that of DMC(0.05).

The photostability of F-2 significantly affects the photo-reactivity of F-2. When F-2 is irradiated with two modules of RUL-3500Å lamps, photosplitting into 8-MOP and thymidine by near 300nm light emitted from the lamp is observed. The breakdown rate is dependent on irradiation time, F-2 decreasing continuously with irradiation time (see Figure 8). While F-2 decreases continuously with irradiation time, F-2-thymidine adducts(biadducts) increases with inflection point, not proportional to disappearance of F-2. This is may be due to the photosplitting of F-2 as expected from appearance of 8-MOP on irradiation. The rapid increase of the slope in the last portion of the biadduct formation curve is observed because 8-MOP and thymidine yielded by photosplitting of F-2 remain properly oriented in a dry film state to form F-2 which then photoreacts with another thymidine

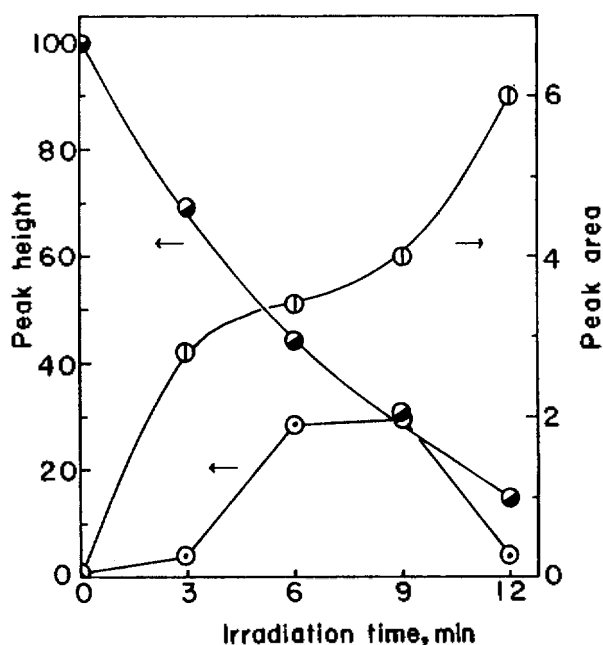
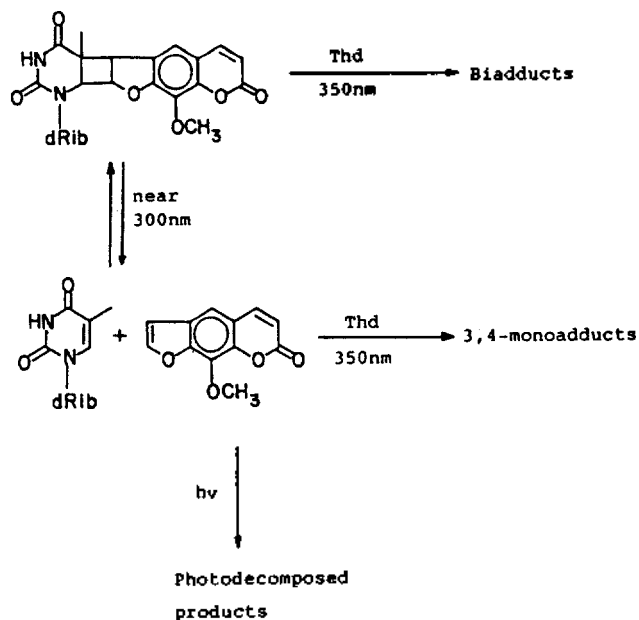


Figure 8. Relative rates of breakdown and biadducts formation of F-2 in a dry film state. ●; F-2, ○; 8-MOP, ◊; biadducts.



Scheme 1. Photoreaction of *cis-syn* 8-MOP<sup>4',5'</sup>Thd with Thymidine in a dry film state.

to produce biadducts. 8-MOP, which is yielded by breakdown of F-2, may also react with another thymidine in proper position to form a 3,4-monoadduct or may be photodecomposed into other compounds. Therefore, the photoreaction of F-2 and thymidine produces many products as shown in Figure 4. However, amount of the products other than biadducts and 8-MOP is relatively small. The photoreaction of F-2 and thymidine in a dry film state is summarized in scheme I.

## Conclusions

The biadduct of 8-MOP and thymidine is first splitted into a 4',5'-monoadduct and thymidine, not into a 3,4-monoadduct and thymidine on exposure to 254nm light. This indicates that cyclobutane ring of pyrone side is photosplitted much faster than that of furan side. Complexation is necessary in C<sub>4</sub>-cycloaddition reaction of F-2 and DMC with thymidine. The rate of DMC-thymidine adduct formation is relatively greater than that of F-2-thymidine adduct formation, *i.e.*, thymidine-8-MOP-thymidine biadduct formation. The steric factor in complexation with thymidine may play an important role in the photoreactivity of F-2 and DMC to thymidine and the photostability of F-2 significantly affects the reactivity of F-2. It is also suggested that the different rate of [2+2] cycloadduct formation is due to the relative reactivity of singlet excited state rather than triplet excited state of both compounds.

**Acknowledgements.** This investigation was supported by the Korea Science and Engineering Foundation and by US PHS Grant Number 5 R01 CA 212729, awarded by the National Cancer Institute, DHHS, U.S.A.

## References

1. L. Musajo, F. Bordin, G. Caporale, S. Marciani, and G. Rigatti, *Photochem. Photobiol.*, **6**, 711 (1967).
2. L. Musajo, F. Bordin, and R. Bevilacqua, *Photochem. Photobiol.*, **6**, 927 (1967).
3. D.M. Kramer and M.A. Pathak, *Photochem. Photobiol.*,

- 12, 333 (1970).
4. D. Kanne, K. Straub, H. Rapoport, and J.E. Hearst, *Biochemistry*, **21**, 861 (1982).
  5. D. Kanne, K. Straub, J.E. Hearst, and H. Rapoport, *J. Am. Chem. Soc.*, **104**, 6754 (1982).
  6. J.A. Parrish, M.D. Thomas, B. Fitzpatrick, L. Tanenbaum, and M.A. Pathak, *New Eng. J. Med.*, **291**, 1207 (1974).
  7. B. Bridge and G. Strauss, *Nature*, **283**, 523 (1980).
  8. C.-N. Ou, P.-S. Song, M.L. Harter, and I.C. Felker, *Photochem. Photobiol.*, **24**, 487 (1976).
  9. M.L. Harter, I.C. Felkner, and P.-S. Song, *Photochem. Photobiol.*, **24**, 491 (1976).
  10. S.C. Shim, H.Y. Koh, and D.Y. Chi, *Photochem. Photobiol.*, **34**, 177 (1981).
  11. S.C. Shim and Y.Z. Kim, *Photochem. Photobiol.*, **38**, 265 (1983).
  12. S.C. Shim and H.K. Kang, *Bull. Korean Chem. Soc.*, **5**, 219 (1984).
  13. S.C. Shim, Y.Z. Kim, and H.K. Kang, *Photochem. Photobiol.*, **40**, 171 (1984).

## The Calculation of Hugoniot Adiabatics and Viscosity of Shock Compressed Water

Dae Hyun Baik and Mu Shik Jhon\*

*Department of Chemistry, Korea Advanced Institute of Science and Technology, Seoul 131*

Byoung Jip Yoon

*Department of Chemistry, Kangreung National University, Kangreung 210. Received April 17, 1986*

The Hugoniot adiabatics and viscosity of shock compressed water have been calculated by applying the significant structure theory of water. To consider the effects of pressure and temperature, the sublimation energy has been expressed by the spherically averaged Stillinger-Rahman ST2 potential. Good agreements between theory and experiment are obtained in the whole extreme ranges of shock wave condition up to 100 GPa (1Mbar).

### Introduction

Along with the development of techniques for shock wave experiments, physical properties of various materials are known for very high pressures and temperatures. Among them liquid water has been studied continuously in various fields of science because of its abnormalities and importances in biological systems. For shock-compressed water, equation of state, electrical conductivity, temperature, velocity of sound, and viscosity have been measured. High explosives have been used to compress water up to 100 GPa (1 Mbar).<sup>1-3</sup> A two-stage light-gas gun has been used to achieve pressures up to 230 GPa (2.3 Mbar).<sup>4</sup> Soviet workers have used strong explosions (presumably nuclear explosions) to reach pressures of 100-3200 GPa (1-32 Mbar).<sup>5,7</sup> The temperature accompanying the shock compression ranges from a few 100°C to several eV (1 eV=11600 K).

The pressure-volume<sup>2,8</sup> and pressure-temperature<sup>9,10</sup> data of shock compression experiments are available for such wide ranges of pressure and temperature for water. Walsh and Rice<sup>2</sup> measured the velocities associated with shock waves by applying the conservation relations.<sup>11,12</sup> The conservation relations for the process are known as Rankine-Hugoniot relations which are

$$P - P_0 = \rho_0 (U_s - U_0) \quad (1)$$

$$V - V_0 (1 - (U_p - U_0)/(U_s - U_0)) \quad (2)$$

$$E - E_0 = \frac{1}{2} (P + P_0) (V_0 - V) \quad (3)$$

where  $P_0$ ,  $\rho_0$ ,  $E_0$ , and  $u_0$  are the initial pressure, density, specific internal energy, and velocity of material, respectively,  $V_0 = 1/\rho_0$  is the initial specific volume,  $P$ ,  $V$ , and  $E$  are, respectively, the final shock pressure, specific volume, and specific internal energy,  $u$ , is the velocity of shock wave, and  $u_p$  is the mass or particle velocity behind the shock front. All of the experimental data from shock compression are convertible into thermodynamic variables using these relations.

Dynamic equation of state data and electrical conductivity for liquid water were obtained in the shock pressure range 30-230 GPa (0.3-2.3 Mbar) using a two-stage light-gas gun by Mitchell and Nellis.<sup>8</sup> With the assumptions of constant  $C$ , and constant  $(\partial P/\partial T)_v$ , Cowperthwaite and Shaw<sup>13</sup> explained the temperature of shock compressed water measured near 200 K and 30 GPa by Kormer.<sup>9</sup> The temperature of shock compressed water have been measured for more wide ranges of temperature and pressure (3300-5200 K and 50-80 GPa) by Lyzenga *et al.*,<sup>10</sup> using a light-gas gun<sup>14</sup> and six channel, time-resolved optical pyrometer.<sup>15</sup> Fairly good agreement between the measured and calculated Hugoniot of water has been obtained by Ree<sup>16</sup> for the temperature range of 1300-3000 K using the perturbation method.

Among various models of liquids, including liquid water as well, the significant structure theory<sup>17,18</sup> is one of the most